J Mol Model (2013) 19:1227–1236
DOI 10.1007/s00894-012-1661-3

ORIGINAL PAPER

Conformational flexibility of the ErbB2 ectodomain and trastuzumab antibody complex as revealed by molecular dynamics and principal component analysis

Juan Felipe Franco-Gonzalez · Victor L. Cruz · Javier Ramos · Javier Martínez-Salazar

Received: 19 June 2012 / Accepted: 22 October 2012 / Published online: 17 November 2012

Abstract Human epidermal growth factor receptor 2 (ErbB2) is a transmembrane oncoprotein that is over expressed in breast cancer. A successful therapeutic treatment is a monoclonal antibody called trastuzumab which interacts with the ErbB2 extracellular domain (ErbB2-ECD). A better understanding of the detailed structure of the receptor-antibody interaction is indeed of prime interest for the design of more effective anticancer therapies. In order to discuss the flexibility of the complex ErbB2-ECD/trastuzumab, we present, in this study, a multi-nanosecond molecular dynamics simulation (MD) together with an analysis of fluctuations, through a principal component analysis (PCA) of this system. Previous to this step and in order to validate the simulations, we have performed a detailed analysis of the variable antibody domain interactions with the extracellular domain IV of ErbB2. This structure has been statically elucidated by x-ray studies. Indeed, the simulation results are in excellent agreement with the available experimental information during the full trajectory. The PCA shows eigenvector fluctuations resulting in a hinge motion in which domain II and C_H domains approach each other. This move is likely stabilized by the formation of H-bonds and salt bridge interactions between residues of the dimerization arm in the domain II and trastuzumab residues located in the C_H domain. Finally, we discuss the flexibility of the MD/PCA model in relation with the static x-ray structure. A movement of the antibody toward the dimerization domain of the ErbB2 receptor is reported for the first time. This finding could have important consequences on the biological action of the monoclonal antibody.

Keywords Extracellular ErbB2 receptor · Herceptin · Molecular dynamics · Principal component analysis · Trastuzumab

Introduction

The human epidermal growth factor receptors (EGFR) HER1 (ErbB1, EGFR), HER2 (ErbB2), HER3 (ErbB3) and HER4 (ErbB4) belong to the family of receptor tyrosine kinase proteins. These receptors are engaged in the regulation of many processes such as cell proliferation, differentiation and apoptosis. Loss of regulation of these receptors has a great impact in a number of human diseases, such as cancer [1, 2].

All EGFR receptors contain three different regions: an extracellular (ectodomain, ECD) ligand-binding region, a single membrane-spanning domain and a cytoplasmatic tyrosine kinase domain. The extracellular EGFR domains have been crystallographically elucidated by several research groups [3–10]. The x-ray structure-based models show the appearance of two large homologous domains (L) and two cysteine-rich domains (CR), in the order L1-CR1-L2-CR2 which is simply known as I-II-III-IV domains, (see Scheme 1).

Electronic supplementary material The online version of this article (doi:10.1007/s00894-012-1661-3) contains supplementary material, which is available to authorized users.

J. F. Franco-Gonzalez · V. L. Cruz (✉) · J. Ramos · J. Martínez-Salazar
BIOPHYM, Macromolecular Physics Department, Instituto de Estructura de la Materia, CSIC, Serrano 113 bis, 28006 Madrid, Spain
e-mail: victor.cruz@iem.cfmac.csic.es

J. F. Franco-Gonzalez
e-mail: felipe.franco@iem.cfmac.csic.es

J. Ramos
e-mail: j.ramos@iem.cfmac.csic.es

J. Martínez-Salazar
e-mail: jmsalazar@iem.cfmac.csic.es

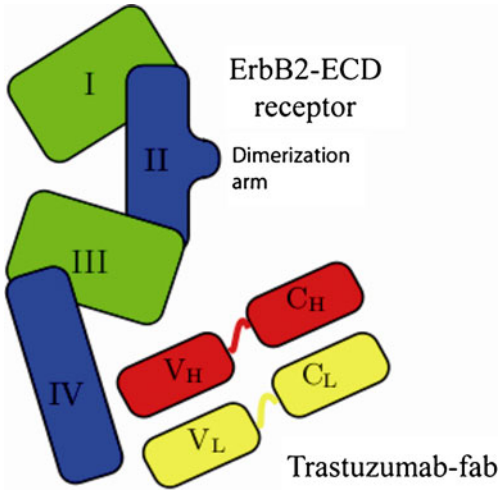

Scheme 1 Schematic representation of the different domains in the ErbB2-ECD/trastuzumab-fab complex. ErbB2-ECD receptor is shown in green (I and III domains) and blue (II and IV domains), whereas trastuzumab, the variable (V) and the conserved domain (C) are represented in yellow (light chain) and red (heavy chain)

The ErbB1, ErbB3 and ErbB4 receptors exhibit a similar tethered structure of the extracellular ligand-binding region when being in the inactive state. Upon ligand activation, a conformational rearrangement from the tethered (inactive) to the extended conformation (active) takes place that permits the homo- and heterodimerization of the receptor through domain II interactions. These active receptor dimers are involved in signaling activity and regulatory protein processes [11, 12]. By contrast, the ErbB2 receptor is characterized by an extended conformation, without ligand binding activation, ready to form dimers with other receptors through an exposed dimerization arm that is located in domain II [3, 8, 12–14]. Thus, over-expression of ErbB2 leads to EGFR receptor activation in tissue culture, while over-expression of other EGFR receptors is not active unless a ligand is added [15].

Trastuzumab, also known as its commercial name Herceptin, currently constitutes a part of the immunotherapy treatment of advanced breast cancers, i.e., those with extensive metastasis, and in general, solid tumors over-expressing ErbB2. Different clinical trials confirm the efficiency of the antibody as an anticancer treatment. The monoclonal antibody trastuzumab can bind to ErbB2-ECD domain [8]. The trastuzumab-fab that binds to domain IV of the ErbB2-ECD categorizes this site as a possible target for anticancer therapies. Additionally, some authors claim, based on these structural studies, that trastuzumab is not effective in blocking dimerization of ErbB2 with ligand activated EGFR or ErbB3 [16, 17]. However it has been reported that ligand independent ErbB2/ErbB3 complex is disrupted by trastuzumab [17]. On the other hand, the Pertuzumab antibody, which binds to domain II (dimerization arm), has shown to be effective to disrupt the ErbB2/ErbB3 ligand activated complex but ineffective for the independent ligand specie. In the light of these findings, it has been hypothesized that the ligand independent interaction between ErbB2/ErbB3 is different from the ligand-induced dimerization. Thus, the domain II-domain II interfaces may not mediate in the ligand-independent complex [17]. In contrast, very recent single-molecule force spectroscopy studies suggest a mechanism of blocking of the heterodimerization of ErbB2/trastuzumab and ErbB3 receptors even in presence of the heregulin (HRG) ligand [18].

Several computational studies based on computer simulations have tackled the structure and interactions between transmembrane ErbB2 domains in lipidic bilayer models [19–24] and in tyrosine kinase domain activation [25–27]. However, computational studies of the interaction of ErbB2 ectodomain (ErbB2 ECD) with antibodies, such as trastuzumab, are less considered. Wang et al. have studied the binding regions of ErbB2 ECD with inhibitory (trastuzumab) and non-inhibitory (HF) monoclonal antibodies using a combination of site-directed mutagenesis, docking and short molecular dynamics simulations. They concluded that the inhibitory trastuzumab antibody binds to domain IV (C-terminal region) of the ECD and that the non-inhibitory HF antibody recognizes domain II (N-terminal region) [28]. In other study, the 3-D structure of an auto-inhibitor (herstatin)/ErbB2 ECD complex has been proposed using molecular docking methods. The binding site of herstatin of the ErbB2 ECD domain was proposed to be at the S1 domain (here domain II). That observation was verified by inmunoprecipitation, confocal microscopy and fluorescence resonance energy transfer experiments [29]. Very recently, Fuentes et al. have published a 20 ns MD study and a fluctuation analysis of the interaction between ErbB2 and a combination of trastuzumab and pertuzumab antibodies [30]. Their simulations throw light on two important aspects of the interaction: on one hand, the fluctuations in domain II are enhanced by the trastuzumab binding, and on the other hand, the existence of a cooperative mechanism between these two antibodies and the ErbB2 ECD that could avoid the homo and heterodimerization of ErbB2 with other members of the EGFR family.

In our work we performed a long 170 ns molecular dynamics (MD) simulations of the ErbB2 ECD/trastuzumab complex (ErbB2/trastuzumab) to elucidate details of the interaction between its components using as starting point the x-ray crystal structure [8]. Additionally, an analysis of the large scale fluctuations has been performed using the principal component analysis (PCA). It should be mentioned here the experimental finding that the variable trastuzumab domains bind to domain IV (juxtamembrane domain) of ErbB2 ECD. These interactions have been largely conserved along the MD simulation. However, large

fluctuations are observed which allow the formation of novel contacts between the dimerization arm of domain II ErbB2 and the trastuzumab residues in the C_H domain. To our best knowledge this interaction has not been yet reported.

Computational methods

Domain nomenclature

The aminoacid sequence intervals are 1–165, 166–310, 311–480 and 481–607 for domain I, II, III and IV of the ErbB2-ECD structure, respectively. The aminoacid sequence intervals of the variable domains of the heavy chain (V_H) and light chain (V_L) of trastuzumab are 1–119 and 1–117, respectively. And finally, the aminoacid sequence intervals of the constant domains of the trastuzumab heavy (C_H) and light (C_L) chains are 127–220 and 114–214 respectively.

Structure modeling

The initial model of the ErbB2 ectodomain and trastuzumab-fab (extra-ErbB2/trastuzumab) was directly taken from the 3-D crystal structure deposited in the Protein Data Bank server (PDB code: 1N8Z) [8]. The missing residues 102–110, 303–305, 361–364 and 581–590 have been modeled based on homologue sequences using the PRODAT database implemented in Sybyl 8.0 [31]. The loop fragment that gave the best geometric fit, based on the homology score and RMS fit, was automatically incorporated into the model [31, 32]. The side chains were built residue by residue, one at a time, using the rotamer library of Sybyl using a scan angle of 30 ° and VDW factor of 0.9. The selected side chain conformation for each modeled residue is the one that presents the fewest VDW contacts with the rest of the molecule. Finally, the structure was relaxed for 2500 steps using the steepest descent minimization algorithm as implemented in GROMACS 4.5.3 [33]. The PROCHECK analysis of the added fragments reports a Ramachandran plot with the following statistics: 64.3 % in most favored regions, 21.4 % in additional allowed regions, 14.3 % in generously allowed regions and 0 % in disallowed regions. From that point of view the structure of the added fragments seems to be quite reasonable.

We assumed that the pKa of the individual amino acid residues at physiological pH does not change when assembled into the protein receptor. Thus, histidine (H) residues remained neutral; lysine (L) and arginine (R) were protonated and aspartic (D) and glutamic (E) acids were deprotonated. The resulting total charge for the complex was −10 e units. The system was solvated by 60,717 water molecules and 10 Na^+ ions have been added to yield an electrically neutral system. Periodic boundary conditions were applied along the three dimensions. The initial rectangular box lengths were 13.9 nm, 12.5 nm and 11.5 nm respectively. The system was equilibrated in a 2 ns NPT-MD simulation with position restraint for all protein atoms.

Molecular dynamics

The OPLS force field [34–36] for protein and the SPC model [37] for water were used along the whole work. Short range repulsion-dispersion interactions were smoothly truncated at 10 Å. The particle mesh Ewald (PME) method [38, 39] was used to calculate long range electrostatic interactions, with a maximum grid spacing of 2.5 Å and using fourth-order (cubic) interpolation for the fast Fourier transforms. The temperature was kept constant at 300 K by coupling the protein, the ions and the solvent independently to an external bath using the Berendsen algorithm [40] with a coupling constant of 0.2 ps.

We used isotropic scaling for the pressure (1 bar). A coupling constant of 1.0 ps and a compressibility of $4.5 \times 10^{-5} bar^{-1}$ were used in the Berendsen algorithm [40]. The dynamics were run using the velocity Verlet integrator, with a time step of 2 fs and bonds constrained conditions using the LINCS algorithm [41].

Production dynamics was performed at constant pressure and temperature (NPT ensemble) releasing all constraints on the heavy atoms during 170 ns and accumulating the trajectory frames every 10 ps. All minimizations, restrained and unrestrained MD runs were performed with GROMACS 4.5.3 [33]. Molecular graphics have been drawn using the VMD 1.8.7 package [42].

Principal component analysis, hydrogen bonds and contact maps

Principal component analysis (PCA) is a method that takes the trajectory of long MD simulations and calculates the dominant modes in the motion of the molecule. Thus, the configurational space is reduced, containing few relevant collective degrees of freedom in which long range fluctuation can be studied [43, 44]. A PCA diagonalizes the covariance matrix of the atom fluctuations from their average trajectory. In this framework, the larger eigenvalues correspond to eigenvectors which explain most of the variance of the atomic fluctuations. The ordering of these eigenvalues gives rise to a small set of modes that capture most of the protein's fluctuations. We have performed a PCA analysis in order to identify the lowest frequency motions occurring in the ErbB2/trastuzumab complex. Along this work, we make use of the first three eigenvectors, which were projected along the MD trajectory. The g_covar and g_anaeig tools

in the GROMACS package were used to perform the PCA analysis.

Hydrogen bond (HB) is considered to exist when both distance between the donor (D) and the acceptor (A) is less than 0.30 nm and the hydrogen-donor-acceptor (HDA) angle is lower than 30 °.

The contact maps show the smallest distance between any pair of atoms belonging to two different residues. The output is a symmetrical matrix of smallest distances between all residues. Plotting these matrices for different time-frames is useful to analyze changes in the structure, and particularly hydrogen bond networks and hydrophobic contacts.

The root-mean square fluctuation for each residue has been calculated using the g_rmsf tool from GROMACS.

The change of secondary structure elements during the simulation was monitored using the program define secondary structure of proteins (DSSP) [45].

Results and discussion

Stability analysis of the full MD trajectory

Figure 1 shows the time evolution of the interaction in the ErbB2-ECD/trastuzumab-fab complex from the MD simulations. At t=0 ns, the initial conformation matches to the x-crystal solved-structure. It is relevant to mention that the secondary structures are well conserved along the whole MD trajectory (see DSSP analysis in the Fig. S1 in the Additional information section). Furthermore, the interaction values between the ErbB2-ECD domain IV and V_H/V_L domains of trastuzumab, which have been experimentally reported, are well preserved during the whole MD trajectory (as will be discussed below). However, after 20 ns, the ErbB2-ECD domain II (dimerization arm) makes contact with the C_H domain of the trastuzumab. Later on, after 100 ns (not shown in Fig. 1), less important contacts between III and V_H domains are found. Most likely, these interactions are a consequence of the driven-contacts between domain II and the C_H domain.

The time evolution of the Cα-RMSD (root mean square deviation) for the ErbB2-ECD receptor has been used to track the equilibration and any possible reorganization of present domains in the whole complex (see Fig. S2 in the Additional information section). The Cα-RMSD relaxes over the first 70 ns to a value of around 0.41±0.03 nm (averaged over the interval 70–170 ns). These structural changes are mainly due to domains IV and II of the ErbB2-ECD, showing the largest values ($C\alpha\text{-RMSD}_{(70ns\text{-}170ns)}$=0.27±0.02 and 0.31±0.04 for domains IV and II, respectively) . On the other hand, Cα-RMSD values for the domains I and III keep stable around 0.12±0.02 nm along the whole trajectory. As shown in Scheme 1 and Fig. 1, the domains II and IV are more exposed to the interaction with the V_L and C_H domains of the antibody structure, respectively.

The ErbB2-ECD residue RMSF values for the x-ray structure (calculated from B factors of the 1N8Z file as $(3B/8\pi^2)^{1/2}$) and for the MD simulations are presented in Fig. 2. As can be seen in the MD simulations, the largest fluctuations are concentrated in the missing loops of the x-ray structure (marked with an asterisk). These large fluctuations are compatible with the fact that these residues cannot be solved in the crystalline structure [8]. Furthermore, several peaks corresponding to the dimerization arm residues (domain II) show large fluctuations (shaded area in Fig. 2), which are well-suited with the movement discussed above. This is in agreement with similar fluctuations of domain II recently observed in shorter MD simulations (20 ns) of the

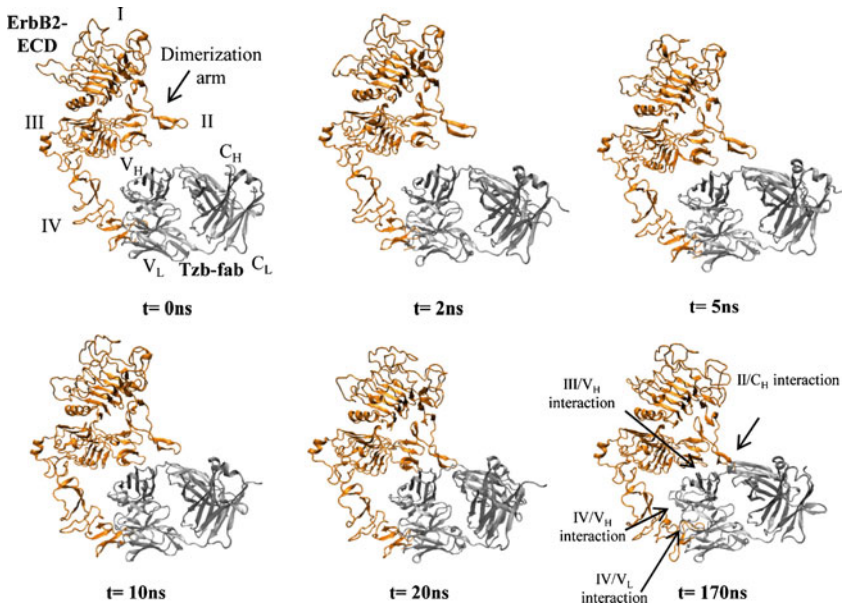

Fig. 1 Selected structures of the ErbB2/trastuzumab complex. Selected snapshots of the ErbB2-ECD/trastuzumab-fab complex along the MD trajectory. The ErbB2-ECD protein and trastuzumab-fab are shown as yellow and blue ribbons, respectively. The configuration at t=0 ns corresponds to the x-ray elucidated structure

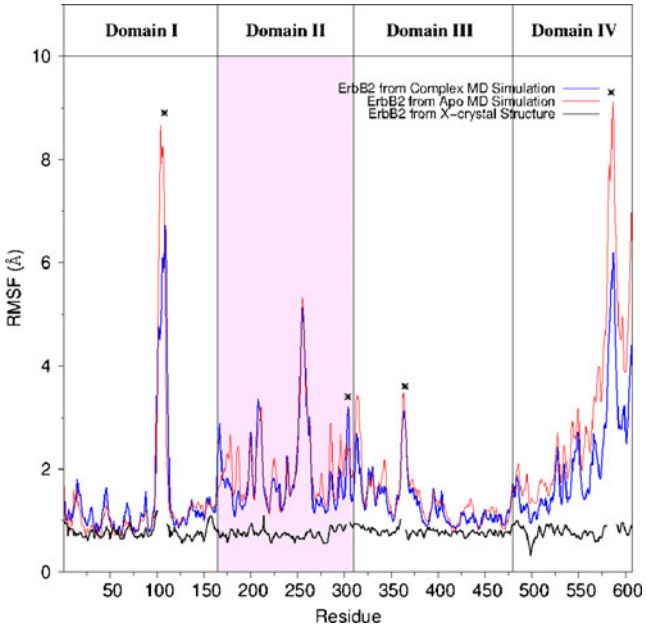

Fig. 2 ErbB2 residue fluctuations along the molecular dynamics. Root mean square fluctuation (RMSF) of backbone atoms of ErbB2-ECD residues from the initial structure (blue line), the apo-protein case (red line) and from the B factors (black line) using the formula $RMSF=(3B/8\pi^2)^{1/2}$. Asterisk stands for missing loops in the x-ray structure 1N8Z. The shaded area indicates residues in domain II

ErbB2-ECD/trastuzumab complex using a different force field [30]. However, these residue fluctuations in the domain II are not observed in the experimental data. This may indicate that the domain II region in the x-ray structure is rather constrained due to the crystalline packing [46, 47]. We will come back to this difference in a subsequent section. We have included in Fig. 2 the RMSF values of the ECD apo-ErbB2 simulation in water to compare with the values corresponding to the ErbB2/trastuzumab complex. As can be observed, the fluctuations in the dimerization arm are very similar in both cases. The main difference between both RMSF profiles corresponds to domain IV, which shows a higher flexibility in the apo-protein case.

Principal component analysis

The PCA allows the projection of the complex protein dynamics on a set of collective modes which can be ordered from the largest to smallest contributions of the protein fluctuation variance, as measured by the eigenvalues of the covariance matrix [43, 44]. The largest eigenvalue corresponds to the slowest motion, and so forth.

The contributions to the motion for the 50 first collective modes are shown in Fig. 3. The major contribution to the collective motion is given by the first nine modes with 90 % of the total protein fluctuations. Modes 1 and 2 contribute

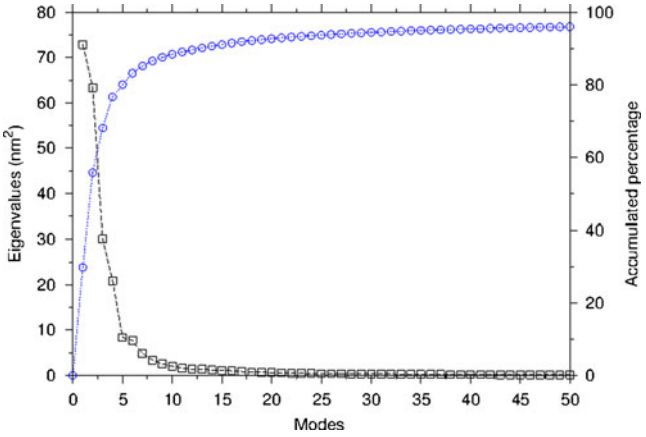

Fig. 3 PCA analysis. Eigenvalues (squares, scale on left side) and accumulated percentage (circles, scale on right side) of the first 50 PCA modes

with 30 and 26 % of the overall motion with fluctuations of 73 and 63 nm^2, respectively. Mode 3 gives 12 % with a fluctuation value of 30 nm^2. These three first modes account for ~70 % of the total protein fluctuations and only the nine first eigenvalues have a value greater than 1 nm^2 (Kaiser criterion discarding eigenvalues below 1) [48] accounting for a 90 % of the total fluctuations.

The three first modes along with the RMSF residue values for each of them are shown in Fig. 4. In the first mode, part of the domain II in ErbB2 translates in a concerted way to domain C_H in the trastuzumab protein. Upon this movement, large fluctuations of the flexible loops (102–110 and 581–590, marked with asterisk) in the domain I and IV are also observed (Fig. 4b, black line). Mode 2 is dominated by the movements of the loop 102–110 in domain I with some minor contributions from a concerted rotational approach of the II and C_H domains of the ErbB2 and trastuzumab proteins (Fig. 4b, red line). Finally, in mode 3, only a torsional combined motion of the II and C_H domains contributes significantly to the overall fluctuation.

These eigenvalues involve large motions of the domain II and C_H motions which can be confirmed by visualizing the distances between the center of mass of the different domains in ErbB2 and trastuzumab moieties. The approach of II and C_H domains is evidenced by a decrease of more than 2 nm of the center of mass distance (CMD). On the other side, the CMD between domain IV in ErbB2 and trastuzumab domains are kept nearly constant throughout the full dynamics and close to those found in the x-ray structure.

In summary, these principal component eigenvector fluctuations result in a hinge motion in which domain II and C_H domains approach each other, allowing the formation of some interactions between the dimerizarion arm in the domain II of ErbB2 protein and the trastuzumab residues

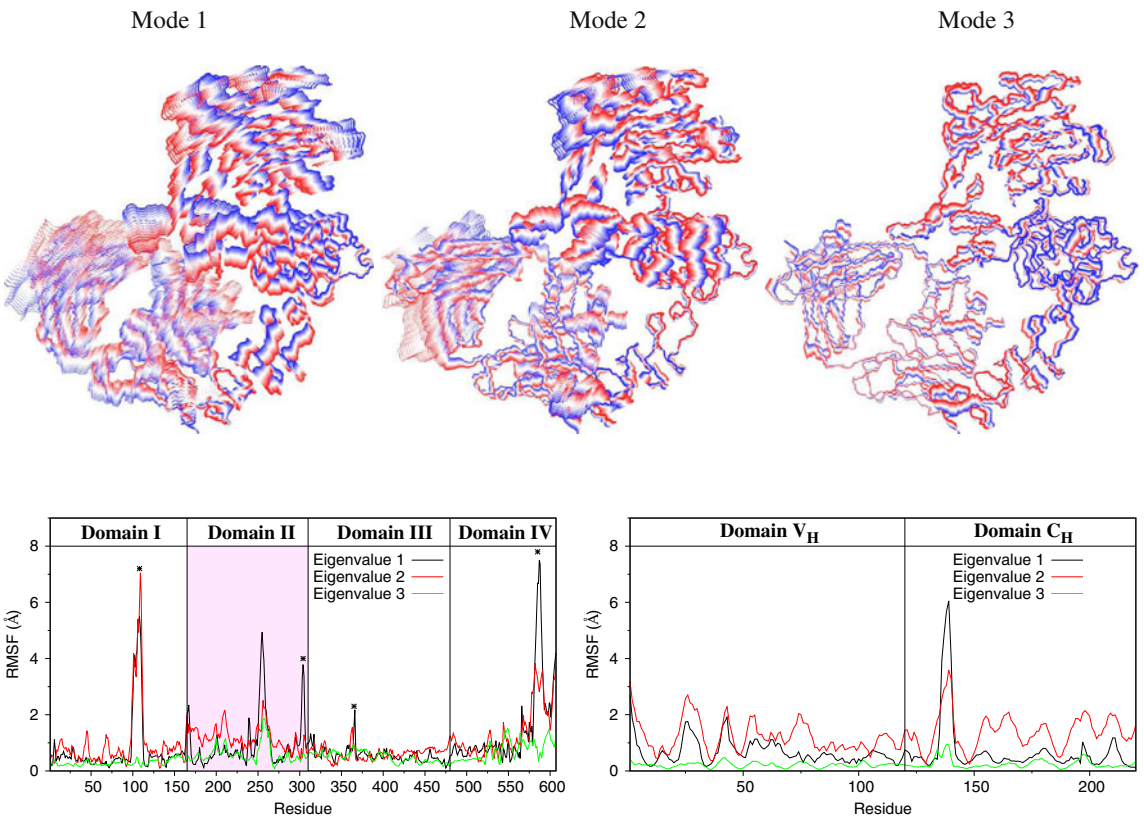

Fig. 4 Eigenvectors from the PCA analysis. **a**) The motion of the three first principal components is overlaid sequentially. Red and blue colors represent large and low-amplitude mode, respectively. The dimerization arm and the Transtuzumab domains exhibit the largest localized motions assisting to the interaction between both regions (see text for details). **b**) Root mean square fluctuation (RMSF) of residues for each mode, 1 (black line), 2 (red line) and 3 (yellow line) in the ERBB2 and trastuzumab proteins. Asterisk stands for missing loops in the x-ray structure 1N8Z. The shaded area indicates residues in domain II of the ERBB2 domain

located in the C_H domain. These interactions will be discussed in the next section.

A detailed analysis of the inter-domain hydrogen bonds and electrostatic interactions between ErbB2 and trastuzumab proteins

Domain IV-V_H/V_L interactions. Comparison with experimental structure

Hydrogen bonds have been characterized according to their residence times during the MD trajectory using the distance and angle criteria defined in the Computational methods section. Firstly, we study the described interactions between domain IV and trastuzumab and compare them with the experimentally available data. Figure 5a shows the time evolution of the hydrogen bonds which describes the interaction of the domain IV of the ErbB2-ECD protein and the domain V_H of the trastuzumab-fab antibody. According to the calculations, three pairs are maintained from the starting structure during the whole simulation, Arg577(IV)-Asp102(V_H), Arg50(V_H)-Glu558(IV) and Arg59(V_H)-Asp560(IV) with occupancies close to 100 %. These interaction pairs can be better considered as salt bridges between charged acidic and basic residues. Similarly, the hydrogen bonds between the domain IV of the ErbB2-ECD protein and the domain V_L of the trastuzumab-fab antibody are shown in Fig. 5b. As can be seen, hydrogen bonds are more labile (small residence time) and they are mainly formed by two pairs, Asn30(V_L)-Gln602(IV), and Thr94(V_L)-Asp560(IV). Furthermore two new H-bonds are alternatively formed by the pair Tyr49(V_L)-Leu586(IV) and Met589(IV)-Tyr49(IV) after 80 ns. All these interactions (Fig. 5c) are in close agreement with the experimental data reported by Cho et al. [8], who showed electrostatic interactions between the 557–560 and 593–603 loops of the ErbB2 ectodomain and the trastuzumab antibody. Hydrophobic interactions have also been described between the loop 570–573 located in the domain IV of the ErbB2 receptor and the trastuzumab-fab antibody in the same experimental work [8]. The hydrophobic interactions were analyzed with the help of the contact map analysis utility which is available at the SPACE server for protein structure analysis (http://ligin.weizmann.ac.il/cma/) [49]. The hydrophobic contacts were selected from the list

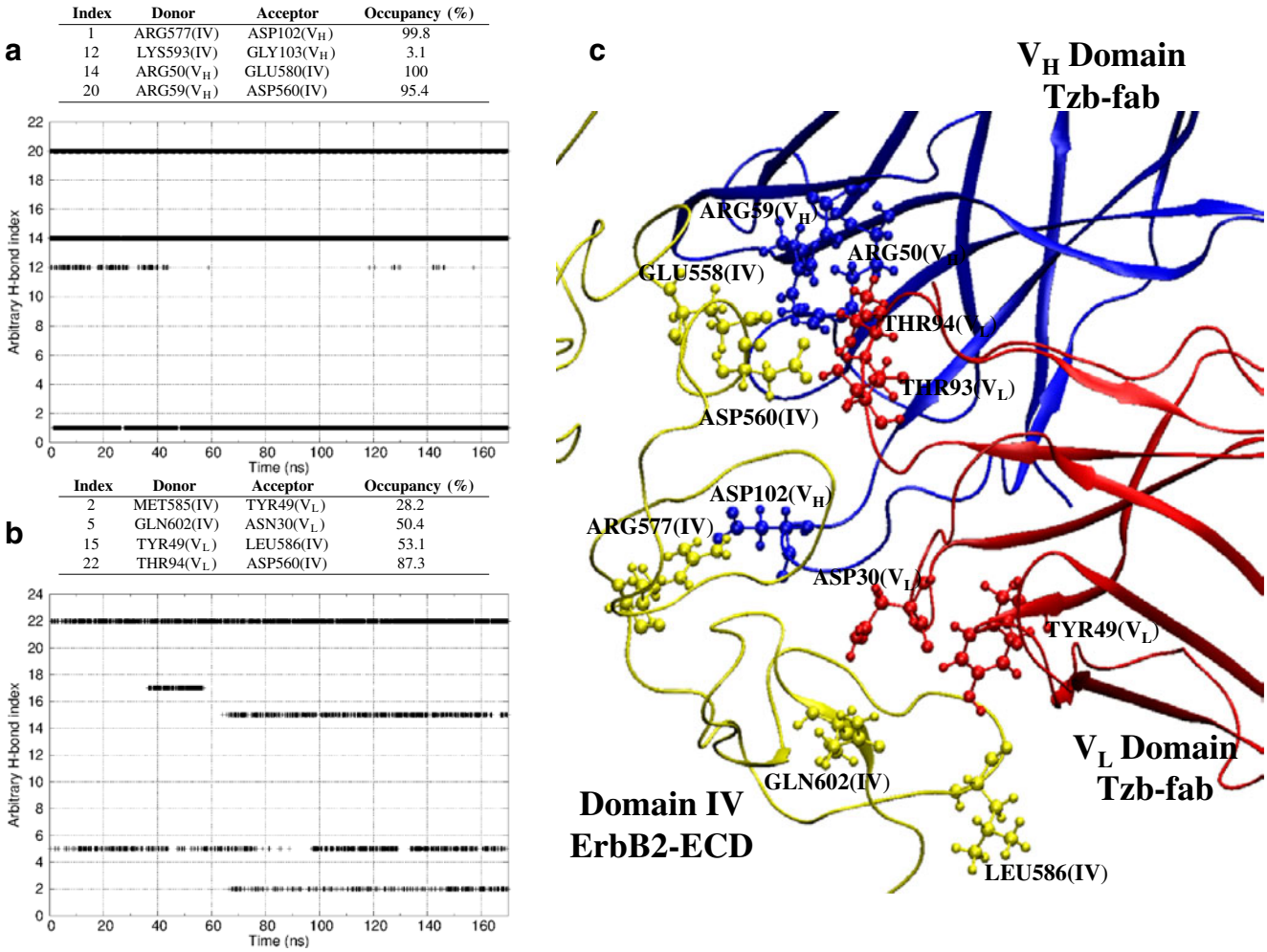

Fig. 5 Hydrogen bond network between antibody and domain IV. **a**) Hydrogen bonds between IV and V_H domains, **b**) Hydrogen bonds between IV and V_L domains and c) Snapshot at 120 ns of the hydrogen bond networks between IV (yellow), V_H (blue) and V_L (red) domains

provided by CMA with two conditions, namely, the contact surface should be above 0.4 nm^2 and the two involved residues should be hydrophobic. Along the MD simulation, the main hydrophobic interactions between these domains are effectively located between the loop 570–573 of the ErbB2 receptor and the hydrophobic CDR3 loop of the V_H subdomain (loop 101–110) in the trastuzumab-fab. In addition, hydrophobic interactions between the 570–573 loop and the CDR3 loop of the V_L domain (loop 93–99) are also observed. Thus, it can be concluded that these hydrogen bond interactions and hydrophobic contacts are very stable, maintaining their distances along the full simulated trajectory.

Domain II-C_H interactions. A possible explanation about the absence of these interactions in the crystal packing structure

Based on the global structural changes observed in the previous section for the domain II, we have investigated possible hydrogen bond interactions and electrostatic contacts with the antibody domains. Figure 6 shows the hydrogen bond network between domain II and C_H region. It can be observed that no hydrogen bonds are presented at the beginning of the simulation. Later on, some residues start forming hydrogen bonds, being the pairs Asn211(C_H)-Thr256(II) and Lys213 (C_H)-Asp255(II) the most stable along the trajectory. The occupancy (fraction of time in which the H-bond is formed) of these H-bonds are 27 % and 74 %, respectively, for the last 70 ns. In the same way, some other electrostatic contacts (in form of salt bridges) have been observed as shown in Fig. S4. Predominantly, a salt bridge between Asp73(V_H) and Lys346 (III) is formed at distances fluctuating between 3.0 and 4.0 Å. The formation of these H-bonds and electrostatic contacts might contribute to stabilize the structure resulting from the hinge motion described above in the PCA analysis, where we stated that the domain II has a large RMSD drift and RMSF values closer to the C_H domain of the antibody.

As shown in the previous paragraph, the dimerization arm is at least as flexible as loops 102–110 and 581–590, which are missed in the x-ray structure indicating its high

Fig. 6 Hydrogen bond network between antibody and domain II. **a**) Hydrogen bonds between II and C_H domains, **b**) Snapshot at 120 ns and zoom of the hydrogen bond networks between II (yellow) and C_H (blue) domains

a

Index	Donor	Acceptor	Occupancy (%)
0	ASN253(II)	ASN211(C_H)	15.5
2	THR256(II)	ASN211(C_H)	13.5
9	LYS208(C_H)	GLU258(II)	9.0
13	ASN211(C_H)	THR251(II)	4.4
14	ASN211(C_H)	THR252(II)	6.7
17	ASN211(C_H)	THR256(II)	13.5
22	ASN211(C_H)	SER259(II)	5.0
30	LYS213(C_H)	ASP255(II)	73.2

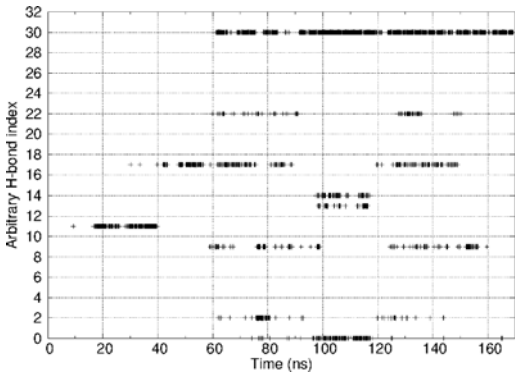

b

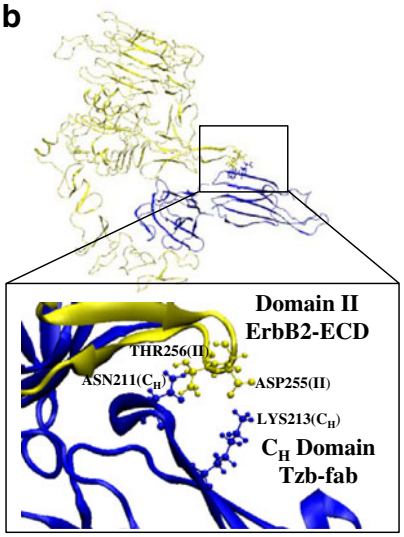

flexibility (Fig. 2). However, the dimerization arm structure has been experimentally solved. A close inspection of the crystallography packing can help to interpret this issue. Figure 7 illustrates two views of the monomer surroundings in the unit cell of the x-ray structure. It can be seen that the dimerization arm is located close to the back-position of a different ErbB2/trastuzumab monomer and interacting with the trastuzumab domain of another different monomer. Thus, both the dimerization arm and the hinge motions are hindered by the closed presence of other monomers in the crystal structure. In our simulations, the lack of other monomers shows evidence of the intrinsic flexibility of the complex ErbB2/trastuzumab, being likely stabilized by H-bond and electrostatic interactions between both components.

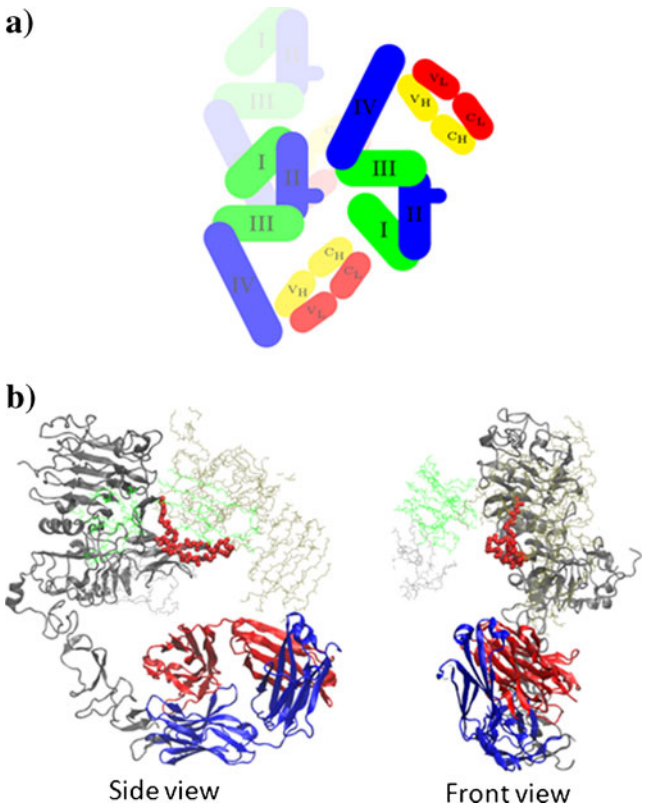

Fig. 7 Crystal packing of the ErbB2/trastuzumab complex. **a**) Schematic representation of the crystal packing of three ErbB2 complexes in 1N8Z. **b**) Front and side views of the 1N8Z crystal packing. Ribbon structure shows an ErbB2/trastuzumab complex along with the nearest spatial neighbor domains represented with lines. The dimerization arm is shown as red VdW spheres

On the other hand, the binding free energy has been calculated according to the molecular mechanics-Poisson-Boltzmann surface area (MM-PBSA) method. The "in-silico" binding energy ΔG_{bind} is quite large (−285.0 kcalmol^{-1}) in comparison with the reported experimental values between −12.4 and −14.0 kcalmol^{-1} [50, 51]. In this sense, Fuentes et al. [30] reported an "in-silico" value of ΔG_{bind}=−1144.6 kcal mol^{-1} using molecular mechanics-generalized-Born surface area (MM-GBSA) approximation without entropic terms. Thus, it seems clear that entropic terms are needed in order to improve the binding energy between the apo-ErbB2 protein and the trastuzumab ligand. Details of the MM-PBSA calculation are given as Supplementary information.

Conclusions

A molecular dynamics and PCA study of the flexibility of the complex between the extracellular domain (ectodomain) of the ErbB2 receptor and the trastuzumab antibody has been presented. The initial structure was prepared from the crystal structure reported by Cho et al. (PDB code: 1N8Z) [8]. From this study the following conclusions can be drawn. Firstly, both secondary structure for the full complex and putative interactions between domain IV of ErbB2 and

variable domains (V_H and V_L) of trastuzumab are well conserved along the molecular dynamics trajectory. Secondly, a hinge move approaching the domain II to the trastuzumab component is revealed by combining the MD trajectory and principal component analysis of the largest eigenvectors. This global motion allows the interaction between the dimerization arm of the ErbB2-ECD domain II and subdomain C_H of the antibody. The effect of this interaction on the heterodimerization of ErbB2 and other EGFR receptors is under study in our group. In addition, we have observed some differences between the MD simulation and the x-ray structure attributed to the crystal packing. Thus, the monomer packing in the crystalline cell hinders the hinge move discussed above due to the presence of two other nearby ErbB2/trastuzumab complexes, thus preventing the interaction between the dimerization arm and the C_H domain of its own trastuzumab protein. In any case, we expect that these results are useful to identify the underlying interaction mechanism between receptor and antibody, which could help to design new therapeutic antibodies. The observed interaction of the antibody with the dimerization arm could provide us with new clues to design possible modifications of the antibody that may then enhance its therapeutic power. An effective blockade of the dimerization arm would impinge the ErbB dimerization and consequently would lead to the interruption of the signaling cascade. The simultaneous effect on both ErbB2 domains II and IV exerted by a modified trastuzumab would be of great interest in the treatment of ErbB2 over-expressed tumors.

Acknowledgments Thanks are due to the, Comision Interministerial de Ciencia y Tecnologia (CICYT) (MAT2009-12364 and MAT2012-36341 projects) for financial support. The authors also acknowledge Secretaria General Adjunta de Informatica- Consejo Superior de Investigaciones Cientificas (SGAI-CSIC) for technical support during the simulations. One of us (J.R) thanks for financial support through the *Ramon y Cajal* program, contract RYC-2011-09585. Very fruitful conversations with Dr. Rafael Nuñez during the discussion of literature experimental details are gratefully appreciated.

References

1. Yarden Y, Sliwkowski MX (2001) Untangling the ErbB signalling network. Nat Rev Mol Cell Biol 2:127–137
2. Wieduwilt M, Moasser M (2008) The epidermal growth factor receptor family: biology driving targeted therapeutics. Cell Mol Life Sci 65:1566–1584
3. Garrett TPJ, McKern NM, Lou M, Elleman TC, Adams TE, Lovrecz GO, Kofler M, Jorissen RN, Nice EC, Burgess AW, Ward CW (2003) The crystal structure of a truncated ErbB2 ectodomain reveals an active conformation, poised to interact with other ErbB receptors. Mol Cell 11:495–505
4. Garrett TPJ, McKern NM, Lou M, Elleman TC, Adams TE, Lovrecz GO, Zhu HJ, Walker F, Frenkel MJ, Hoyne PA, Jorissen RN, Nice EC, Burgess AW, Ward CW (2002) Crystal structure of a truncated epidermal growth factor receptor extracellular domain bound to transforming growth factor-a. Cell 110:763–773
5. Ogiso H, Ishitani R, Nureki O, Fukai S, Yamanaka M, Kim JH, Ogiso H, Ishitani R, Nureki O, Fukai S, Yamanaka M, Kim JH (2002) Crystal structure of the complex of human epidermal growth factor and receptor extracellular domains. Cell 110:775–787
6. Ferguson KM, Berger MB, Mendrola JM, Cho HS, Leahy DJ, Lemmon MA (2003) EGF activates its receptor by removing interactions that autoinhibit ectodomain dimerization. Mol Cell 11:507–517
7. Cho HS, Leahy DJ (2002) Structure of the extracellular region of HER3 reveals an interdomain tether. Science 297:1330–1333
8. Cho HS, Mason K, Ramyar KX, Stanley AM, Gabelli SB, Denney DW Jr, Leahy DJ (2003) Structure of the extracellular region of HER2 alone and in complex with the Herceptin fab. Nature 421:756–760
9. Lu C, Mi LZ, Grey MJ, Zhu J, Graef E, Yokoyama S, Springer TA (2010) Structural evidence for loose linkage between ligand binding and kinase activation in the epidermal growth factor receptor. Mol Cell Biol 30:5432–5443
10. Bouyain S, Longo PA, Li S, Ferguson KM, Leahy DJ (2005) The extracellular region of ErbB4 adopts a tethered conformation in the absence of ligand. Proc Natl Acad Sci USA 102:15024–15029
11. Baselga J, Swain SM (2009) Novel anticancer targets: revisiting ErbB2 and discovering ErbB3. Nat Rev 9:463–475
12. Burgess AW, Cho HS, Eigenbrot C, Ferguson KM, Garrett TPJ, Leahy DJ, Lemmon MA, Sliwkowski MX, Ward CW, Yokoyama S (2003) An open-and-shut case? Recent insights into the activation of EGF/ErbB receptors. Mol Cell 12:541–552
13. Hynes NE, Lane HA (2005) ErbB receptors and cancer: the complexity of targeted inhibitors. Nat Rev Cancer 5:341–354
14. Vicente-Alique E, Núñez-Ramírez R, Vega JF, Hu P, Martínez-Salazar J (2011) Size and conformational features of ErbB2 and ErbB3 receptors: a TEM and DLS comparative study. Eur Biophys J 40:835–842
15. DiFiore PP, Pierce JH, Segatto O, King CR, Aaronson SA (1987) ErbB-2 is a potent oncogene when overexpressed in NIH/3T3 cells. Science 237:178–182
16. Agus DB, Akita RW, Fox WD, Lewis GD, Higgins B, Pisacane PI, Lofgren JA, Tindell C, Evans DP, Maiese K, Scher HI, Sliwkowski MX (2002) Targeting ligand-activated ErbB2 signaling inhibits breast and prostate tumor growth. Cancer Cell 2:127–137
17. Junttila TT, Akita RW, Parsons K, Fields C, Phillips GDL, Friedman LS, Sampath D, Sliwkowski MX (2009) Ligand-independent HER2/HER3/PI3K complex is disrupted by trastuzumab and is effectively inhibited by the PI3K inhibitor GDC-0941. Cancer Cell 15:429–440
18. Shi X, Xu L, Yu J, Fang X (2009) Study of the inhibition effect of herceptin on interaction between heregulin and ErbB receptors HER2/HER3 by single-molecule force spectrsocopy. Exp Cell Res 315:2847–2855
19. Garnier N, Genest D, Genest M (1996) Correlated motions and propagation of the effect of a local conformational change in the transmembrane helix of the c-ErbB2 encoded protein and in its V659E mutant, studied by molecular dynamics. Biophys Chem 58:225–237
20. Samma Soumana O, Aller P, Garnier N, Genest M (2005) Transmembrane peptides from tyrosine kinase receptor. Mutation-related behavior in a lipid bilayer investigated by molecular dynamics simulations. J Biomol Struct Dyn 23:91–100
21. Duneau JP, Genest D, Genest M (1996) Detailed description of an alpha helix->pi bulge transition detected by molecular dynamics simulations of the p185(c-ErbB2) V659G transmembrane domain. J Biomol Struc Dyn 13:753–769
22. Garnier N, Crouzy S, Genest M (2003) Molecular dynamics simulations of the transmembrane domain of the oncogenic ErbB2 receptor dimer in a DMPC bilayer. J Biomol Struc Dyn 21:179–199

23. Samma Soumana O, Garnier N, Genest M (2008) Insight into the recognition patterns of the ErbB receptor family transmembrane domains: heterodimerization models through molecular dynamics search. Eur Biophys J 37:851–864
24. Bocharov EV, Mineev KS, Volynsky PE, Ermolyuk YS, Tkach EN, Sobol AG, Chupin VV, Kirpichnikov MP, Efremov RG, Arseniev AS (2008) Spatial structure of the dimeric transmembrane domain of the growth factor receptor ErbB2 presumably corresponding to the receptor active state. J Biol Chem 283:6950–6956
25. Telesco SE, Radhakrishnan R (2008) Atomistic insights into regulatory mechanisms of the HER2 tyrosine Kinase domain: a molecular dynamics study. Biophys J 96:2321–2334
26. Shih AJ, Telesco SE, Cho SH, Lemmon MA, Radhakrishnan R (2011) Molecular dynamics analysis of conserved hydrophobic and hydrophilic bond-interaction networks in ErbB family kinases. Biochem J 436:241–251
27. Telesco SE, Shih AJ, Jia F, Radhakrishnan R (2011) A multiscale modeling approach to investigate molecular mechanisms of pseudokinase activation and drug resistance in the HER3/ErbB3 receptor tyrosine kinase signaling network. Mol Biosyst 7:2066–2080
28. Wang JN, Feng JN, Yu M, Xu M, Shi M, Zhou T, Yu XD, Shen BF, Guo N (2003) Structural analysis of the epitopes on ErbB2 interacted with inhibitory or non-inhibitory monoclonal antibodies. Mol Immunol 40:963–969
29. Hu P, Feng J, Zhou T, Wang J, Jing B, Yu M, Hu M, Zhang X, Shen B, Guo N (2005) In vivo identification of the interaction site of ErbB2 extracellular domain with its autoinhibitor. J Cell Physiol 205:335–343
30. Fuentes G, Scaltriti M, Baselga J, Verma CS (2011) Synergy between trastuzumab and pertuzumab for human epidermal growth factor 2 (Her2) from colocalization: an in silico based mechanism. Breast Cancer Res 13:1–9
31. SYBYL 8.0, Tripos International, 1699 South Hanley Rd., St. Louis, MO, 63144, USA
32. Dayhoff MO, Schwartz RM, Orcutt BC (1978) Atlas of protein sequence and structure. National Biomedical Research Foundation, Washington, DC
33. Hess B, Kutzner C, van der Spoel D, Lindahl E, GROMACS 4 (2008) Algorithms for highly efficient, load-balanced, and scalable molecular simulation. J Chem Theory Comp 4:435–447
34. Jorgensen WL, Tirado-Rives J (1988) The OPLS [optimized potentials for liquid simulations] potential functions for proteins, energy minimizations for crystals of cyclic peptides and crambin. J Am Chem Soc 110:1657–1666
35. Jorgensen WL, Tirado-Rives J (2005) Chemical theory and computation special feature: potential energy functions for atomic-level simulations of water and organic and biomolecular systems. J Proc Natl Acad Sci USA 102:6665–6670
36. Kaminski GA, Friesner RA, Tirado-Rives J, Jorgensen WL (2001) Evaluation and reparametrization of the OPLS-AA force field for proteins via comparison with accurate quantum chemical calculations on peptides. J Phys Chem B 105:6474–6487
37. Berendsen HJC, Postma JPM, van Gunsteren WF, Hermans J (1981) In: Pullman B (ed) Intermolecular forces. Reidel, Dordrecht, The Netherlands, pp 331–342
38. Darden T, York D, Pedersen L (1993) Particle mesh Ewald: An N·log(N) method for Ewald sums in large systems. J Chem Phys 98:10089–10092
39. Essmann U, Perera L, Berkowitz ML, Darden T, Lee H, Pedersen LG (1995) A smooth particle mesh Ewald method. J Chem Phys 103:8577–8593
40. Berendsen HJC, Postma JPM, Vangunsteren WF, Dinola A, Haak JR (1984) Molecular dynamics with coupling to an external bath. J Chem Phys 81:3684–3690
41. Hess B, Bekker H, Berendsen HJC, Fraaije J, LINCS (1997) A linear constraint solver for molecular simulations. J Comput Chem 18:1463–1472
42. Humphrey W, Dalke A, Schulten K, VMD (1996) Visual molecular dynamics. J Mol Graphics 14:33–38
43. Amadei A, Linssen AB, Berendsen HJ (1993) Essential dynamics of proteins. Proteins 17:412–425
44. Amadei A, Linssen AB, de Groot BL, van Aalten DM, Berendsen HJ (1996) An efficient method for sampling the essential subspace of proteins. J Biomol Struct Dyn 13:615–625
45. Kabsch W, Sander C (1983) Dictionary of protein secondary structure: pattern recognition of hydrogen-bonded and geometrical features. Biopolymers 22:2577–2637
46. Lou H, Cukier RI (2006) Molecular dynamics of apo-adenylate kinase. A principal component analysis J. Phys. Chem B 110: 12796–12808
47. Hunenberger PH, Mark AE, Van Gunsteren WF (1995) Fluctuation and cross-correlation analysis of protein motions observed in nanosecond molecular-dynamics simulations. J Mol Biol 252:492–503
48. Kaiser HF (1960) The application of electronic-computers to factor-analysis. Educ Psychol Meas 20:141–151
49. Sobolev V, Eyal E, Gerzon S, Potapov V, Babor M, Prilusky J, Edelman M (2005) SPACE: a suite of tools for protein structure prediction and analysis based on complementarity and environment. Nucl Acids Res 33:W39–W43
50. Troise F, Cafaro V, Giancola C, D'Alessio G, Lorenzo C (2008) Differential binding of human immunoagents and Herceptin to the ErbB2 receptor. FEBS J 275:4967–4979
51. Bostrom J, Haber L, Koenig P, Kelley RF, Fuh G (2011) High affinity antigen recognition of the dual specific variants of herceptin is entropy-driven in spite of structural plasticity. PLOS 6(4):e17887